Manipulation of protein-complex function by using an engineered heterotrimeric coiled-coil switch†

Toshihisa Mizuno,*[a] Kumiko Suzuki,[a] Tatsuya Imai,[a] Yuya Kitade,[a] Yuji Furutani,[a] Motonori Kudou,[b] Masayuki Oda,[c] Hideki Kandori,[a] Kouhei Tsumoto[b] and Toshiki Tanaka*[a]

Received 19th January 2009, Accepted 15th May 2009
First published as an Advance Article on the web 18th June 2009
DOI: 10.1039/b901118h

Design methodology of variant proteins, in which original functions can be manipulated by additive ligand binding, is an attractive target of protein engineering. Especially for multi-protein complexes, techniques for constructing variants which allow the switching on or off of original functions by ligands have been limited until now. We examined a method of utilizing a *de novo* designed protein module, **IZ-DS**, which has a tertiary structure that can be significantly changed from a random coil to a folded coiled-coil structure following binding with peptide ligand, **IZ-3K**. By introducing a metamorphosis **IZ-DS** sequence to one of the components in a target multi-protein complex, the **IZ-3K** binding and the subsequent structural transition of the **IZ-DS** moiety would affect the tertiary structure of the introduced protein unit, and the function of the total multi-protein complex may also be altered. In this research, we used the T7 RNA polymerase (T7 RNAP)/T7 lysozyme complex as the target multi-protein complex, in which allosteric binding of the T7 lysozyme to T7 RNAP halts the RNA synthesis of T7 RNAP. The **IZ-DS** sequence was introduced to the T7 lysozyme. By optimizing the introduction site of the **IZ-DS** sequence in the T7 lysozyme, we succeeded in constructing the T7 lysozyme variant, **DS-Lys^{23}**. In the absence of **IZ-3K**, the mixture of T7 RNAP and **DS-Lys^{23}** exhibited RNA synthesis due to the weakening of the interaction between T7 RNAP and **DS-Lys^{23}**. Whereas, after the addition of **IZ-3K**, RNA synthesis was significantly suppressed by the binding of **DS-Lys^{23}/IZ-3K** complex. The present methodology using a designed ligand-dependent metamorphosis protein sequence constitutes another possible method for the *de novo* manipulation of various functions of natural protein complexes.

Introduction

Methods of constructing recombinant proteins, in which original functions are manipulated with desirable external stimuli such as ions,[1] pH,[2] photo-irradiation,[3] or ligand binding,[4] are an attractive target of protein design. In particular, applying these proteins to functional macromolecules, such as sensor proteins and ligand-dependent enzymes (*in vivo* or *in vitro*), tuning their functions with external specific ligands is quite a versatile technique. For this objective, conjugating the ligand-binding site from a natural receptor with the target protein has been widely performed and has received a good assessment of its feasibility.[5] Although such combination proteins sometimes exhibit elegant success in endowing ligand-dependency,[6] there have only been a few successful cases. One of the main reasons, perhaps, is that the tertiary structures of most natural ligand-binding domains are not significantly changed by ligand binding. Such small structural-alteration sometimes fails with a weak perturbation for the target protein structures introduced. Thus, the fluctuation of functions before and after ligand-binding is insignificant. In order to endow various target proteins with a ligand-dependent characteristic, a ligand-binding protein module in which the tertiary structure can be significantly altered by specific ligand binding would be necessary.

Recently, we have been engaged in the *de novo* design of coiled-coil proteins, in which 2–7 amphiphilic α-helical peptides are wrapped together in a superhelical manner, having 3.5 amino acids per turn.[7] Following simple interactions, and the easier prediction of tertiary structure from the designed amino acid sequences, the coiled-coil proteins were studied for the design of *de novo* protein structures and functions. First, we designed a sequence, YGG(IEKKIEA)$_4$, [*d,e,f,g,a,b,c*] designated as **IZ**,[8] where three **IZ** peptides assembled into a stable parallel homo-trimeric α-helical coiled-coil structure. Since the hydrophobic packing at the *a* and *d* positions is quite important for keeping the coiled-coil proteins in a bundled-structure, a small number of mutations of the *a* and/or *d* positions significantly influences their thermal stability.[9] Replacing one Ile at the *a* position of the second heptad of **IZ** with a Trp, **IZ-2aW**, or an Ala, **IZ-2aA**, results in the bundled structures of both **IZ-2aW** and **IZ-2aA** becoming destabilized.[10] By adding extra mutations at their *f* positions, **IZ-2aW(fQ)** and **IZ-2aA(fA)** take a random coil structure.[11] On the other hand, they form an

[a]*Graduate School of Engineering, Nagoya Institute of Technology, Gokiso-cho, Showa-ku, Nagoya 466-8555, Japan. E-mail: toshitcm@nitech.ac.jp, ttanaka@nitech.ac.jp; Fax: +81-52-735-5237; Tel: 81-52-735-5237*
[b]*Graduate School of Frontier Science, Department of Medical Genome Science, University of Tokyo, 5-1-5 Kashiwanoha, Kashiwa, Chiba 277-8562, Japan*
[c]*Graduate School of Life and Environmental Sciences, Kyoto Prefectural University, 1-5 Hangi-cho, Shimogamo, Sakyo-ku, Kyoto 606-8522, Japan*
† This paper is dedicated to the inspiring work of Prof. Seiji Shinkai on the occasion of his 65th birthday.

AAB-type hetero-trimeric coiled-coil structure, consisting of one **IZ-2aW** (or **IZ-2aW(fQ)**) and two **IZ-2aA** (or **IZ-2aA(fA)**). The size-complement effect in the hydrophobic packing of the side-chains, by one indole ring and two methyl groups, significantly contributes to the specificity of their assembly.

These drastic structural transitions, from random coil to coiled-coil structure, encouraged us to tune the tertiary structure of the natural enzyme. First, we applied the idea to the RNA hydrolysis enzyme, RNaseT1.[12] By introducing two **IZ-2aA(fA)** sequences at each end of the circular permutant RNaseT1, its enzymatic activity for RNA hydrolysis was initially markedly suppressed, but was recovered by binding with **IZ-2aW(fQ)**. The folding of two **IZ-2aA(fA)** with one **IZ-2aW(fQ)** into the trimeric coiled-coil structure would induce the refolding of the RNaseT1 moiety. Thus a ligand peptide-triggered switch of enzyme activity was performed. Following the same concept, we succeeded in constructing a metal-ion dependent GFP, by combining the metal-ion triggered trimeric coiled-coil with a circular permutated GFP.[13] Using such designed metamorphosis proteins allowed us to fabricate stimuli-dependent protein variants.

In this paper, we demonstrate the aforementioned strategy for tuning the function of multi-protein complexes. In nature, most proteins assemble and cooperatively, or sometimes interferingly, execute individual functions. In order to broaden our understanding of the modulation of such multi-protein systems, we examined the effect of the folding regulation of one of the components of a protein complex on the functions of the total protein complex. The alteration of one of the protein structures could affect the interaction with its counterparts. That, in turn, could affect the functional activity of the total protein complex.

According to procedures used in our previous work, the target proteins to be endowed with ligand-dependency required circular permutation[14] due to the suppression of their original functions before the addition of ligand. However, since the distances between the N- and C-termini of more than half of the natural single domain proteins are not within 20 Å,[15] circular permutation would restrict the applicability of our concept. Therefore, we designed a new coiled-coil module, **IZ-DS**, having two amphiphilic helical peptides and a flexible linker connecting them. This sequence can be inserted as a "ligand-triggered metamorphosis linker" instead of a linked peptide chain. After the addition of the counterpart helical peptide **IZ-3K** as a ligand, its structure is transformed from a random coil to a folded coiled-coil structure, accompanying the **IZ-3K** binding. Thus, the structure of the original protein, which is destabilized by the introduction of an unfolded **IZ-DS** sequence, would be recovered for the sake of the folding of the **IZ-DS** moiety, and then the function of the original protein could be turned on. This module should be helpful if introduced into most natural proteins or protein-complexes.

On the other hand, we chose a T7 RNAP/T7 lysozyme complex[16] as the target multi-protein complex for this study. T7 lysozyme is known to bind with T7 RNAP and suppress the RNA synthesis of T7 RNAP due to inhibition of the conformational change of T7 RNAP from the initiation complex to the elongation complex onto the promoter. This allosteric interaction is performed on the surface between T7 lysozyme and T7 RNAP, and thereby, a small fluctuation of the T7 lysozyme structure may affect this allosteric interaction, resulting in the manipulation of RNA synthesis by T7 RNAP. By optimizing the introduction site of the **IZ-DS** sequence, we succeeded in constructing its variant, **DS-Lys^{23}**. Using a general *in vitro* RNA synthesis protocol, we examined the alteration of the RNA synthesis activity of the **DS-Lys^{23}**/T7 RNAP complex before and after the addition of the ligand peptide **IZ-3K** and succeeded in regulating the RNA synthesis (Scheme 1).

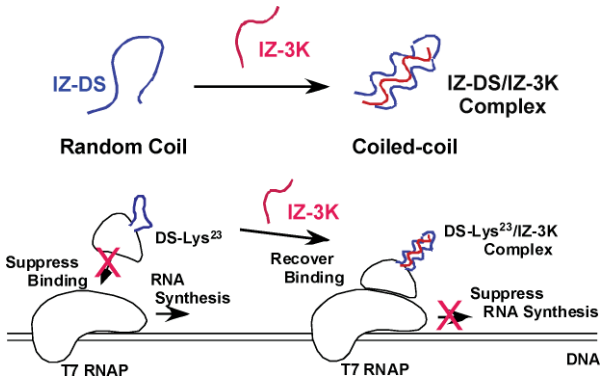

Scheme 1 Schematic illustration of the ligand-induced switch of the protein-complex function.

Results and discussion

Design of 2 + 1 heterotrimeric α-helical coiled-coil

Recently, we have been engaged in the design of α-helical coiled-coil proteins, especially for trimeric α-helical coiled-coils. First, we designed the peptide sequence, YGG(IEKKIEA)$_4$, **IZ**,[8] forming a parallel homotrimeric α-helical coiled-coil structure. By mutating several Ile residues at the *a* and/or *d* positions with other amino acids, pH-dependent coiled-coils,[17] metal-ion-dependent coiled-coils,[18] and AAB- and ABC-type heterotrimeric coiled-coils[10,11] were successfully constructed. In the case of the AAB-type heterotrimeric coiled-coil, the Ala-Ala-Trp interaction, instead of the Ile-Ile-Ile in **IZ**, at the *a* position of the second heptad repeat generated a heterogeneous interaction at the hydrophobic core and permitted the selective assembly of three different **IZ**-based mutant-peptides, having Ala or Trp at the *a* position. Although each α-helical peptide adopted a random coil structure, they assembled into the trimeric coiled-coil structure, only by mixing at a 2:1 ratio. This selective assembly, accompanying marked structural transition from a random coil to a coiled-coil structure, may be an effective way of modulating the tertiary structure of various natural proteins, allowing protein activity to be switched on or off. By connecting two **IZ-2aA(fA)** sequences (A-type peptide) to the N- and C- termini of the circular permutant RNaseT1, the binding of **IZ-2aW(fQ)** (B-type peptide) exhibited a significant increase in RNaseT1 activity.[12] The newly generated terminal ends of the target protein resulting from the construction of the circular permutant could be brought close enough together to refold and recover the original structure with the aid of the AAB-type trimeric coiled-coil assembly. With this strategy, however, circular permutation of the target protein is necessary, which restricts the applicability of the designed metamorphosis peptide sequences that respond to ligand peptides. Therefore, we aimed to create another peptide sequence, which responds to

an externally added peptide, that permits simple insertion into various natural protein sequences without circular permutation.

A type of "ligand-triggered metamorphosis linker",[19] in which the tertiary structure is significantly changed by ligand binding, was postulated to be a prominent candidate for this objective, since this peptide sequence could be easily inserted into various natural proteins instead of a linked peptide chain.[20] Changing the tertiary structure of a "ligand-triggered metamorphosis linker" by ligand binding could markedly affect the conjugated target protein structure, and thus the fluctuations of the protein's function before and after ligand binding would increase. To this end, we first designed the 2 + 1 heterotrimeric coiled-coil, referring to the previously designed AAB-type trimeric coiled-coil.[10,11] The sequences are illustrated in Fig. 1. **IZ-AA** consists of two α-helical peptides, both with one Ala mutation instead of Ile at

IZ-AA

defgabc defgabc defgabc defgabc
IEQKIEA IEQKAEA IEQKIEA IEQKIEA
cbagfed cbagfed cbagfed cbagfed
AEIEQKI AEIEQKA AEIEQKI AEIEQKI
Linker

Linker : GGTGGG

IZ-W

defgabc defgabc defgabc defgabc
IEQEIEA IKQEIEA WKQKIEA IKQEIEA

IZ-DS

defgabc defgabc defgabc defgabc
IEQKIEA IEQKDEA IEQKIEA IEQKIEA
cbagfed cbagfed cbagfed cbagfed
AEIEQKI AEIEQKS AEIEQKI AEIEQKI
Linker

Linker : GGTGGG

IZ-3K

defgabc defgabc defgabc defgabc
IEAKIAA IEAKIAA KEAKIAA IEAKIAA

IZ-2K

defgabc defgabc defgabc defgabc
IEAKIAA IEAKKAA IEAKIAA IEAKIAA

DC

cdefg abcdefg abcdefg abcdefg ab
QLEDK IEELLSK IYHLENE IARLKKL IG
cdefg abcdefg abcdefg abcdefg ab
QLEDK IEELLSK IYHLENE IARLKKL IG
Linker

Linker : EGGTGG

IZ-A4

defgabc defgabc defgabc defgabc
IEQKIEA IEQKAEA IEQKAEA IEQKIEA
cbagfed cbagfed cbagfed cbagfed
AEIEQKI AEIEQKA AEIEQKA AEIEQKI
Linker

Linker : GGTGGG

Fig. 1 The amino acid sequences of **IZ-AA**, **IZ-W**, **IZ-DS**, **IZ-3K**, **IZ-2K**, **DC**, and **IZ-A4**.

the *a* or *d* position, and a flexible linker, GGTGGG, connecting them, while **IZ-W** consists of one α-helical peptide with one Trp mutation at the *a* position instead of Ile. In order to avoid the formation of homo-trimeric or -polymeric bundled structures by themselves, all *f* positions in **IZ-AA** and **IZ-W** were replaced by a Gln. The Gln mutation at the *f* positions reduces interaction among the α-helical peptides in the coiled-coil,[21] which means we could expect increases in interaction specificity between them. The *e* positions of the first α-helical peptide and the *g* positions of the second α-helical peptide in the **IZ-AA** were occupied by a Glu, while the *g* positions of the first α-helical peptide and the *e* positions of the second α-helical peptide were occupied by Lys. In **IZ-W**, the *e* positions were occupied by Glu and the *g* positions by Lys. After the formation of a 1:1 complex, they formed a trimeric α-helical coiled-coil structure, having a salt-bridge interaction between the *e* and *g* positions of each helix and Ala-Ala-Trp interaction at the hydrophobic core. The CD spectra of **IZ-AA** and **IZ-W** and a 1:1 mixture of the two are shown in Fig. 2(a). **IZ-AA** seemed to form an α-helical structure even in the absence of **IZ-W**. The two α-helical peptides in **IZ-AA** alone cannot make a dimeric or polymeric bundled structure, but connection with a linker sequence should reinforce the interaction between them despite the weakening of the hydrophobic interaction by the Ala mutation. In contrast, **IZ-W** alone takes a random coiled structure. After mixing **IZ-AA** and **IZ-W** in a 1:1 ratio, a slight increase of the helicity compared with that of **IZ-AA** was observed. This suggests that an assembly of **IZ-AA** with **IZ-W** would form a trimeric coiled-coil structure. Increases in the T_m values observed in the presence of 2 M urea, from >50 °C for **IZ-AA** to 56 °C for the 1:1 mixture of **IZ-AA** and **IZ-W**, also supported the heterogeneous 1:1 binding (Fig. 2(c)). But an intramolecular interaction of two α-helical peptides in **IZ-AA**, forming a coiled-coil-like structure, was not suitable for the current purpose as a ligand-triggered metamorphosis linker. Thus we designed a different 2 + 1 heterotrimeric coiled-coil using another interaction at the hydrophobic core.

IZ-DS is composed of two α-helical peptides and a 6-residue linker, GGTGGG, which connects them. In **IZ-DS**, the *a* position of the second heptad repeat of the first helical peptide is Asp, and the *d* position of the third heptad repeat of the second helical peptide is Ser. In order to decrease the interaction between the α-helical peptides in **IZ-DS**, the *f* positions of the first and second helical peptides were replace by a Gln. **IZ-3K**, based likewise on the **IZ** sequence, has a Lys at the *d* position of the third heptad repeat. To prevent the formation of the homotrimer of **IZ-3K**, the *f* positions were occupied by an Ala, referring to the design concept in **IZ-2aA(fA)**.[11] The *e* positions of the first α-helical peptide and the *g* positions of the second α-helical peptide in **IZ-DS** were occupied by Glu, while the *g* positions of the first α-helical peptide and the *e* positions of the second α-helical peptide were occupied by Lys. In **IZ-3K**, the *e* positions were occupied by a Glu and the *g* positions were occupied by Lys. After the formation of a 1:1 complex, it is possible that they form a trimeric α-helical coiled-coil structure, having a salt-bridge interaction of Glu and Lys between the *e* and *g* positions of each helix and a salt-bridge interaction of Lys and Asp at the hydrophobic core. We performed the CD spectral measurements for 10 μM of **IZ-DS**, **IZ-3K** and a 1:1 mixture of the two in 20 mM Tris HCl buffer (pH 7.5) containing 50 mM NaCl; these results are illustrated in Fig. 2(b).

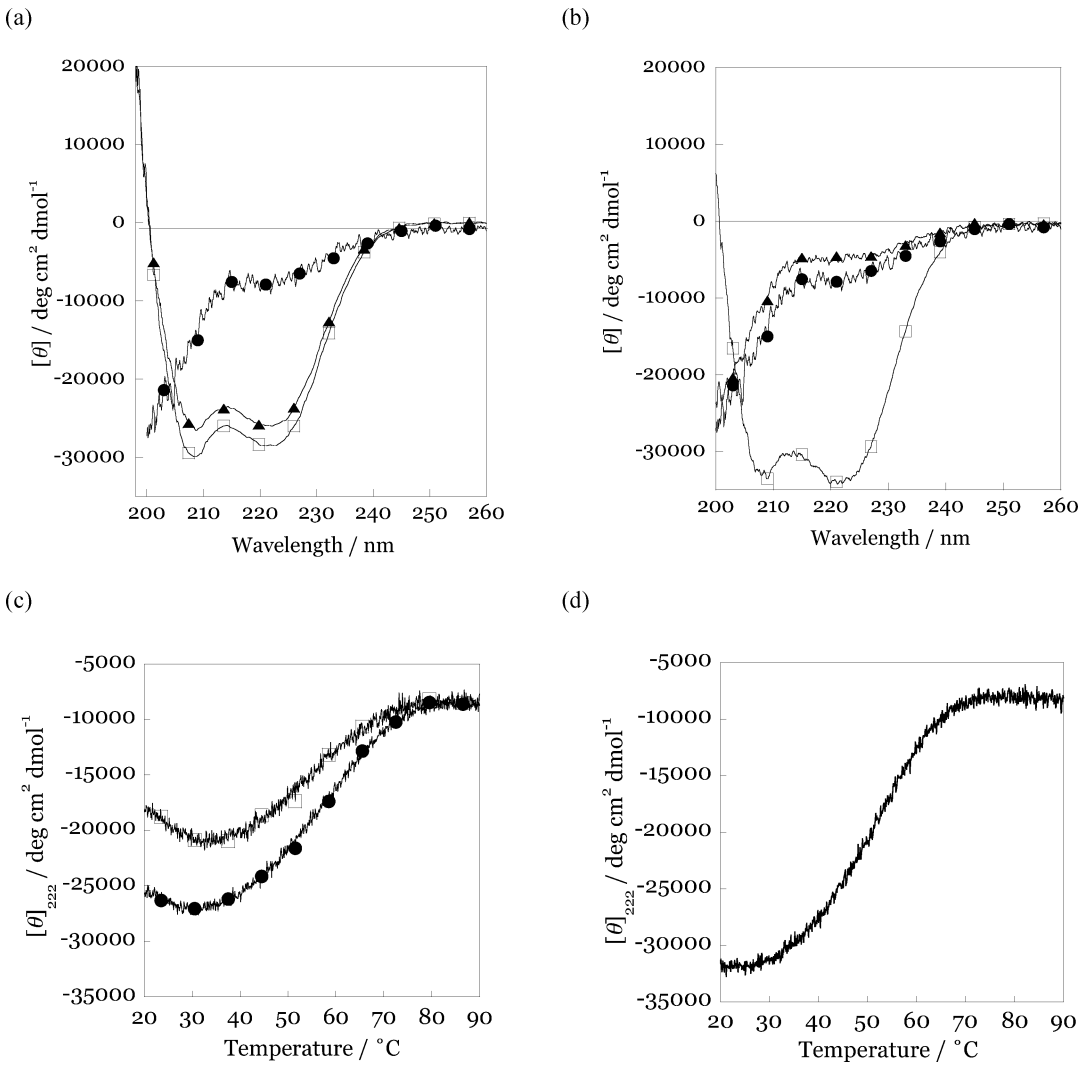

Fig. 2 (a) CD spectra of **IZ-W** (●), **IZ-AA** (▲) and 1:1 complex of **IZ-W/IZ-AA** (□); [protein] = 10 μM, 20 mM Tris HCl (pH 7.5), 50 mM NaCl, 25 °C. (b) CD spectra of **IZ-3K** (●), **IZ-DS** (▲) and 1:1 complex of **IZ-3K/IZ-DS** (□); [protein] = 10 μM, 20 mM Tris HCl (pH 7.5), 50 mM NaCl, 25 °C. (c) Temperature dependence of $[\theta]_{222}$ of **IZ-AA** (□) and **IZ-W/IZ-AA** complex (●) in the presence of 2 M urea; [protein] = 10 μM, 20 mM Tris HCl (pH 7.5), 50 mM NaCl, 1 °C/min. (d) Temperature dependence of $[\theta]_{222}$ of **IZ-DS/IZ-3K** complex; [protein] = 10 μM, 20 mM Tris HCl (pH 7.5), 50 mM NaCl, 1 °C/min.

Both **IZ-DS** and **IZ-3K** showed CD spectra with $[\theta]$ minima less than 200 nm, corresponding to a random coil structure, while the 1:1 mixture showed $[\theta]$ minima at 208 and 222 nm, typical for an α-helical structure. The ratio of $[\theta]_{222}/[\theta]_{208}$ was 1.03, supporting an α-helical coiled-coil structure. The $[\theta]_{222}$ changes of **IZ-DS** by the addition of **IZ-3K** showed a clear flexion point at a 1:1 ratio of **IZ-DS** and **IZ-3K**, indicating 1:1 binding between them (data not shown). The T_m value of the **IZ-DS/IZ-3K** complex was estimated at 58 °C from the temperature dependence of $[\theta]_{222}$ based on the two-state folding model (Fig. 2(d)).

In order to support the formation of electrostatic interaction between Asp and Lys at the hydrophobic core, we observed the IR spectra of a carboxyl group in the Asp residue. IR spectroscopy of the carbonyl group is quite a good indicator for examining the protonated or deprotonated state of carboxylic groups in the protein scaffold. Generally, in the deprotonated state, the IR bands corresponding to the symmetrical and asymmetrical vibrations are observed at 1650–1540 cm^{-1} and 1450–1360 cm^{-1}, respectively, and at 1780–1705 cm^{-1} in the protonated state.[22] We measured the IR spectrum of a 1:1 mixture of **IZ-DS/IZ-3K** (total concentration of protein was 300 μM or 1.5 mM) in a solution of 50 mM phosphate buffer (pH 7.0 or 3.0) containing 100 mM NaCl, as shown in Fig. 3. Although the carboxyl groups of Glu from **IZ-DS** and **IZ-3K** also show the IR bands for the deprotonated species at 1565 cm^{-1} (asymmetric stretch) and 1403 cm^{-1} (symmetric stretch), the IR band corresponding to the protonated species was not observed at pH 7.0. When the pH was decreased to 3.0, the protonated carboxyl group band was observed at 1723 cm^{-1} with a concomitant decrease of the IR bands from the deprotonated forms (Fig. 3(a) and 3(c)). **IZ-DS** has 16 Glu residues and one Asp residue, and **IZ-3K** has four Glu residues; therefore, a total of 21 carboxyl groups exist in the **IZ-DS/IZ-3K** complex. Among them, only the Asp residue in **IZ-DS** is designed to interact with the Lys residue in **IZ-3K** through the interhelical

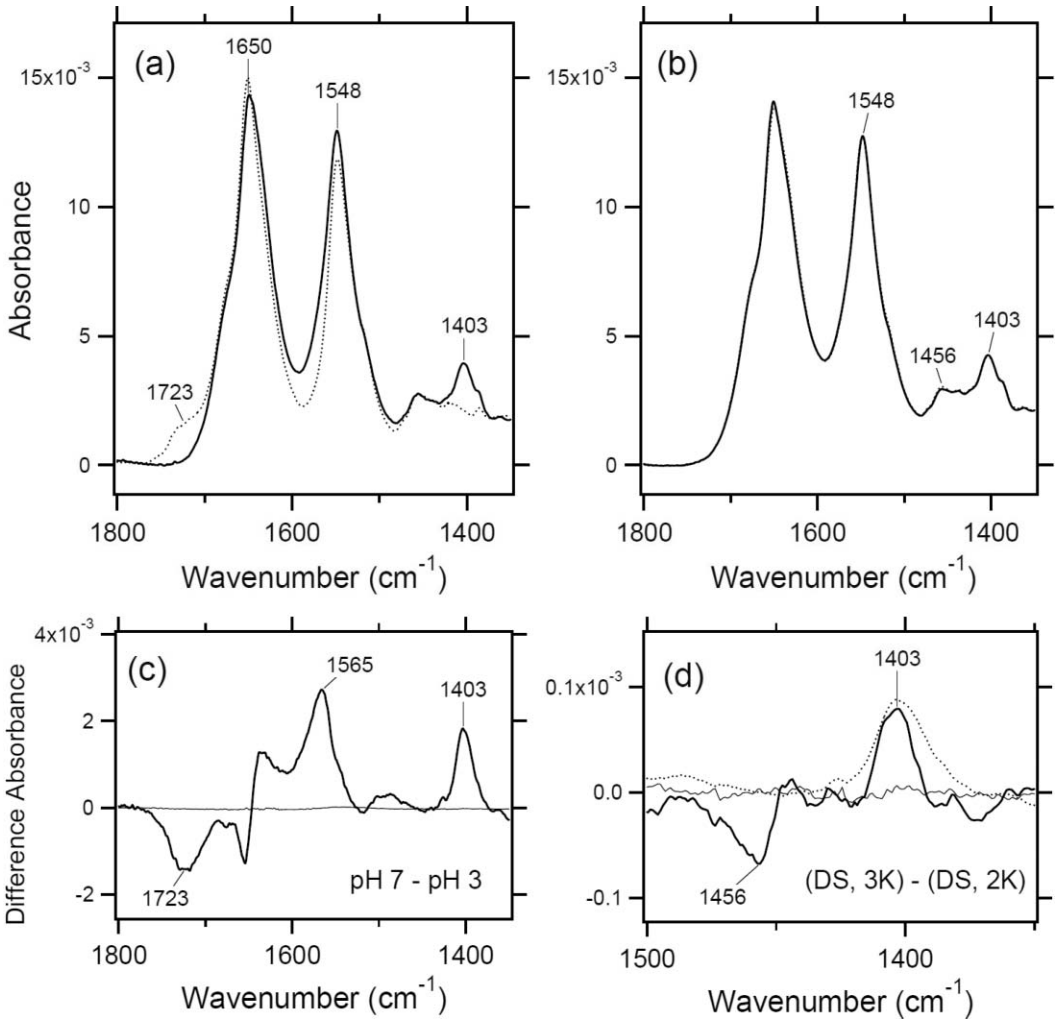

Fig. 3 (a) IR spectra of the **IZ-DS/IZ-3K** complex; [protein] = 300 μM, 50 mM sodium phosphate (pH 7.0 (solid line) or 3.0 (dotted line)), 100 mM NaCl, 23 °C. The bands at 1650 and 1548 cm^{-1} are assigned to the amide I and II modes, respectively. (b) IR spectra of **IZ-DS/IZ-3K** (solid line) and **IZ-DS/IZ-2K** (dotted line) complexes; [protein] = 1.5 mM, 50 mM sodium phosphate (pH 7.0), 100 mM NaCl, 23 °C. The spectra were normalized at the 1548 cm^{-1} band (amide II) (normalization factor of 0.25). (c) Difference spectra between the solid and dotted spectra in (a). (d) Difference spectra between the solid and dotted spectra in (b). The dotted line is reproduced from (c) with reduction of different absorbance to one twenty-first, which corresponds to the infrared absorption from one deprotonated carboxyl group. The thin line in (c, d) represents baseline distortion caused by thermal fluctuation and sample exchange.

hydrophobic space. To examine the interaction between Asp and Lys residues, we compared the IR spectra of the **IZ-DS/IZ-3K** and **IZ-DS/IZ-2K** complexes. The sequence of **IZ-2K** is shown in Fig. 1. **IZ-3K** has a Lys at the *d* position of the third heptad repeat, while **IZ-2K** has a Lys at the *a* position of the second heptad repeat. The frequency of the carboxyl group of the Asp residue in **IZ-DS** should be different depending on the manner of interaction with the Lys residue, which is located at different positions in **IZ-3K** and **IZ-2K**. In Fig. 3(a), two large bands at 1650 and 1548 cm^{-1} originate from amide bonds in the polypeptide, which are called amide I and II modes, respectively. To clarify the vibrational bands of deprotonated and protonated carboxyl groups in the peptide, we calculated the difference spectrum in Fig. 3(c). Fig. 3(d) shows the different spectra of **IZ-DS/IZ-3K** and **IZ-DS/IZ-2K** complexes, in which a positive band at 1403 cm^{-1} and a negative band at 1456 cm^{-1} are probably assigned to the symmetric vibration of the deprotonated carboxyl group of the Asp residue. The frequency of the 1456 cm^{-1} band of the **IZ-DS/IZ-2K** complex was unusually higher than that reported in the literature, suggesting an unknown interaction between the carboxyl group of the Asp with other residues, although the total similarity between the IR spectra of both complexes indicates that they retain a similar trimeric coiled-coil structure. Also, the frequency of the 1403 cm^{-1} band from the **IZ-DS/IZ-3K** complex was similar to those of other carboxylic groups in the **IZ-DS/IZ-3K** complex. The absorbance at 1403 cm^{-1} in Fig. 3(d) corresponded to one twenty-first, compared with that in Fig. 3(c), suggesting that the absorbance of the 1403 cm^{-1} band in Fig. 3(d) corresponds to one Asp in the **IZ-DS/IZ-3K** complex. To support the differences of interaction between Lys and Asp residues in the **IZ-DS/IZ-3K** and **IZ-DS/IZ-2K** complexes, we compared their T_m values, calculated from their temperature dependence $[\theta]_{222}$ shown in Fig. 4. The T_m values were estimated at 58 °C for **IZ-DS/IZ-3K** and 42 °C for **IZ-DS/IZ-2K**. This result would indicate that there was a more effective

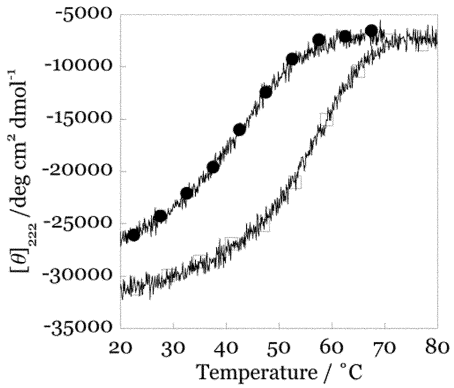

Fig. 4 Temperature dependence of $[\theta]_{222}$ of **IZ-DS/IZ-3K** (□) and **IZ-DS/IZ-2K** (●) complexes; [**IZ-DS**] = 2.5 μM, [**IZ-3K** or **IZ-2K**] = 2.5 μM, 20 mM Tris HCl (pH 7.5) containing 50 mM NaCl, 25 °C.

interaction between Lys and Asp in **IZ-DS/IZ-3K** than **IZ-DS/IZ-2K**.

By means of ATR-FTIR spectroscopy, we determined that the carboxyl group of Asp is in the deprotonated form in the hydrophobic area of the **IZ-DS/IZ-3K** complex. Meanwhile, our previous work on **IZ-2aE**[17a] and the work by Tripet *et al.*[9] suggest that the placement of a negatively-charged residue at the hydrophobic core results in serious destabilization with respect to the coiled-coil formation; thus the neighboring cationic species from Lys would interact and lessen this unfavorable effect. As a result, the electrostatic interaction at the hydrophobic core prevented the self-assembly of **IZ-DS** and **IZ-3K**, and instead, enabled a hetero-assembly between them. The pair **IZ-DS** and **IZ-3K** were considered to be suitable as a ligand-triggered metamorphosis linker sequence and a ligand peptide for the current objective.

Choosing an optimized site on the T7 lysozyme for the insertion of metamorphosis IZ-DS sequence

In order to manipulate T7 RNAP activity by tuning the tertiary structure of T7 lysozyme by the ligand-triggered metamorphosis **IZ-DS** sequence, we attempted to discern the optimal site for insertion of **IZ-DS**. Since fluctuation of the T7 lysozyme structure is performed by structurally altering the **IZ-DS** moiety by **IZ-3K** binding, we first used the folded dimeric coiled-coil as a substitute for the folded state of **IZ-DS**, induced by the complex with **IZ-3K**. The dimeric coiled-coil, **DC**, was constructed by connecting two α-helical peptides based on the GCN4-pIL-based sequences[23] with a flexible linker, EGGTGG, giving a single-chain dimeric coiled-coil (Fig. 1). The CD spectrum of **DC** (10 μM) in 20 mM Tris HCl (pH 7.5) buffer, containing 50 mM NaCl, indicated a typical α-helical shape with spectral minima at 208 and 222 nm. The ratio of $[\theta]_{222}/[\theta]_{208}$ was about 1.0 for the coiled-coil structure (data not shown), and its T_m value was over 95 °C. Using **DC**, we first chose the most tolerant site for incorporation, without losing the tertiary structure and the inhibition activity of the T7 lysozyme moiety for T7 RNAP.

T7 lysozyme is composed of 151 amino acids, forming five α-helices and 12 β-sheets. For binding to T7 RNAP, its N-terminal areas, such as Ala[2], Arg[3], Val[4] and Gln[5], and α-helix 1, ranging from Val29 to Glu39, serve as important residues and a detailed structural examination has been confirmed using crystallographic analysis.[16] T7 lysozyme binds to the surface area opposite the active-site cleft for RNA synthesis in T7 RNAP, and this is therefore an indirect mechanism of inhibition. Thinking of this mechanism, three sites in the T7 lysozyme, between Pro[23] and Ser[24], Glu[62] and Met[63], and Lys[70] and Gly[71], were selected as candidates able to receive **DC** (Fig. 5), and their characteristics were examined accordingly. Three conjugated proteins were produced by the *E. coli* BL21(DE3) strain, and their solubilities were examined by analyzing each supernatant and precipitant fraction by sodium dodecylsulfate polyacrylamide electrophoresis (SDS-PAGE), respectively. The conjugates with **DC** between Glu[62] and Met[63], and Lys[70] and Gly[71] mainly appeared in the precipitant fraction, while the one with **DC** between Pro[23] and Ser[24] was observed in the supernatant, suggesting that this conjugate did not suffer a significant loss of tertiary structure. We named this conjugate **DC-Lys**[23] and subsequently examined its inhibition activity for T7 RNAP. Inhibition activity was measured using the standard *in vitro* RNA production system. In order to avoid non-specific interactions among T7 lysozymes with template DNA or the produced RNA *etc.* due to the cationic charges of the T7 lysozyme, 0.01 wt% BSA was added as a dummy protein in the enzyme reaction. Upon the addition of **DC-Lys**[23] to the T7 RNAP solution, the RNA synthesis of T7 RNAP was clearly suppressed. From the titration analyses of **DC-Lys**[23] for the RNA synthesis reaction, we determined an IC_{50} value of 0.5 μM, which is about 5-fold weaker than that of wild-type T7 lysozyme (Fig. 6 and Table 1).

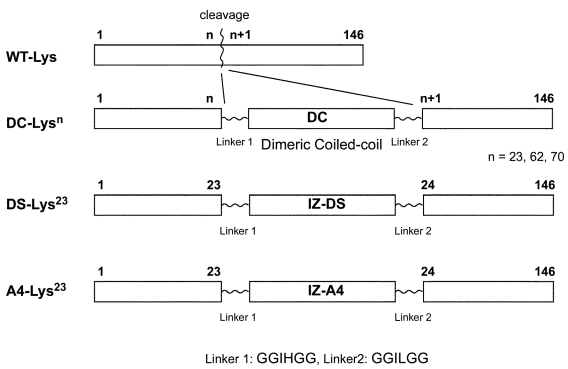

Fig. 5 Schematic illustrations of the T7 lysozyme variants.

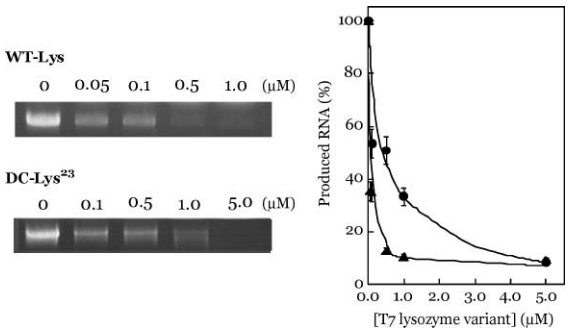

Fig. 6 The inhibition of RNA synthesis of T7 RNAP by **WT-Lys** (▲) and **DC-Lys** (●); [T7 lysozyme variant] = 0–5 μM, T7 RNAP 5 u, 20 mM rNTP, 10 mM DTT, 2 mM spermidine, 0.01 wt% BSA, 20 mM HEPES (pH 7.9), reaction time 2 hours.

Table 1 IC_{50} of lysozyme variants

T7 Lysozyme variants	IC_{50} (μM)
WT-Lys	0.1
DC-Lys^{23}	0.5
DS-Lys^{23}	>50[a]
DS-Lys^{23} + **IZ-3K**	7.0

[a] Due to the solubility of **DS-Lys**^{23}, we could not determine the exact value.

On the other hand, **IZ-A4**, has the same peptide-length as **IZ-AA** but takes a random coiled structure due to the extra Ala mutations instead of Ile at the *a* position of the third heptad repeat of the first α-helical peptide and the *d* position of the second heptad repeat of the second α-helical peptide of **IZ-AA**. In **A4-Lys**^{23}, **DC** in **DC-Lys**^{23} was substituted with **IZ-A4** sequence, and we examined its inhibition activity for T7 RNAP. **IZ-A4** was used as the substitute of an unfolded **IZ-DS**. From the SDS-PAGE analysis, **A4-Lys**^{23} was observed in the supernatant fraction, suggesting that its tertiary structure was retained, but the inhibition activity for the RNA synthesis was diminished, even with the addition of more than 200 μM of this conjugate. The CD spectrum of **A4-Lys**^{23} shown in Fig. 7 supported a destabilized protein structure, due to the insertion of an unstructured **IZ-A4** sequence. Consequently, the site between Pro^{23} and Ser^{24} should be a position well suited for switching the T7 RNAP activity by transformation of the **IZ-DS** moiety.

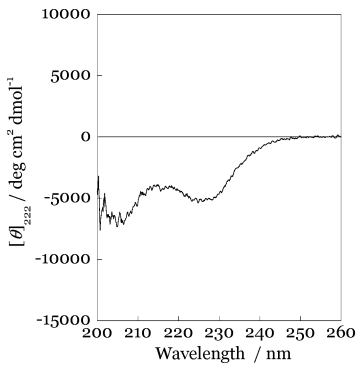

Fig. 7 CD spectrum of **A4-Lys**^{23}; [**A4-Lys**^{23}] = 2.5 μM, 20 mM Tris HCl (pH 7.5) containing 50 mM NaCl, 25 °C.

Construction of the IZ-DS-conjugated T7 lysozyme and its inhibition activity for the RNA synthesis of T7 RNAP

We constructed the **IZ-DS**-conjugated T7 lysozyme variant by exchanging the **IZ-DC** sequence of **DC-Lys**^{23} with the **IZ-DS** sequence and named it **DS-Lys**^{23}. First, we examined the CD spectral changes of **DS-Lys**^{23} upon the addition of **IZ-3K** to observe the binding behavior, as shown in Fig. 8. Before the addition of **IZ-3K**, the CD spectrum of **DS-Lys**^{23} (10 μM) in 20 mM Tris HCl (pH 7.5) containing 50 mM NaCl, indicated a mixed spectrum, supposedly composed of those with destabilized T7 lysozyme with a partially folded **IZ-DS** sequence. Following the addition of **IZ-3K** to **DS-Lys**^{23}, the CD values at 208 and 222 nm, typical for the α-helix formation, were decreased and saturated at addition of one equivalent of **IZ-3K**. The **IZ-3K**

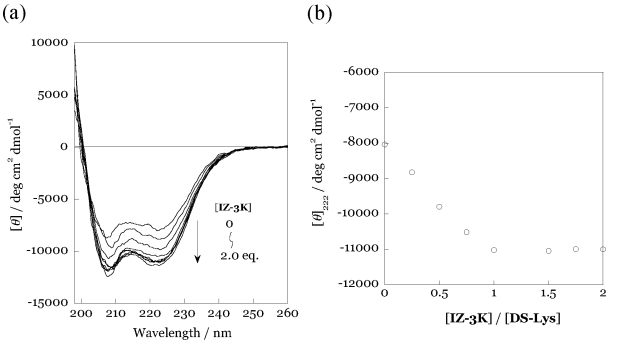

Fig. 8 (a) CD spectral changes of **DS-Lys**^{23} upon the addition of **IZ-3K**, (b) $[\theta]_{222}$ changes of **DS-Lys**^{23} upon the addition of **IZ-3K**; [**DS-Lys**^{23}] = 2.5 μM, [**IZ-3K**] = 0–5.0 μM, 20 mM Tris HCl (pH 7.5) containing 50 mM NaCl, 25 °C.

binding and the subsequent coiled-coil formation at the **IZ-DS** moiety of **DS-Lys**^{23} should mainly contribute to these spectral changes; thus the flexibility of **IZ-DS** moiety would still be maintained. The 1:1 complex of **DS-Lys**^{23} with **IZ-3K** intimates a precise recognition of the **IZ-DS** moiety for **IZ-3K**. Meanwhile, the structural alteration of the **IZ-DS** moiety, evaluated from the CD spectral change of **DS-Lys**^{23} by **IZ-3K** seems to be smaller than that of the complex of **IZ-DS** with **IZ-3K** (Fig. 2(b)). This may be caused by a tendency to maintain the original folding of the T7 lysozyme moiety, and it may help to bring the edge of the introduced helical peptides of the **IZ-DS** sequence close enough to promote the formation of a dimeric coiled-coil-like structure; although only **IZ-DS** takes a random coil structure.

The detailed binding affinity of **DS-Lys**^{23} with **IZ-3K** was analyzed using surface plasmon resonance (SPR) measurement. **IZ-3K** was biotinylated at the N-terminal *via* biotin-polyethyleneglycol-EGGG linker and immobilized onto an avidin-coated sensor chip, SA (Biacore). Following injection of the **DS-Lys**^{23} solution onto this sensor chip, an SPR signal, corresponding to the **DS-Lys**^{23} binding, was observed. From the titration analyses of **DS-Lys**^{23}, we obtained a K_d value of 244 nM. As a control experiment, we observed the binding of **IZ-DS** using the same sensor chip and obtained a K_d value of 308 nM. These comparable affinities also indicate that the inserted **IZ-DS** moiety in **DS-Lys**^{23} would maintain its flexibility without losing its binding ability for **IZ-3K**, and that this structural alteration would be expected to induce a perturbation of the T7 lysozyme scaffold.

Next, the effect of **IZ-3K** binding to **DS-Lys**^{23} on the RNA synthesis of T7 RNAP was examined using the same standard RNA production conditions. The results are shown in Fig. 9. Although the addition of 20 μM **DS-Lys**^{23} showed a slight decrease in RNA synthesis, the subsequent addition of 20 μM of **IZ-3K** indicated an effective decrease in RNA synthesis. From the curve fitting analyses of Fig. 9(b), the IC_{50} for **DS-Lys**^{23} was evaluated to be higher than 50 μM, while that for **DS-Lys**^{23} + **IZ-3K** was 7.0 μM. Although the recovered inhibition activity was about 1.4%, compared with that of the wild-type T7 lysozyme, a successful restoration of T7 lysozyme activity by the **IZ-3K** binding was realized.

Using isothermal titration calorimetry (ITC) measurement, we attempted to evaluate the binding constant of T7 RNAP with T7

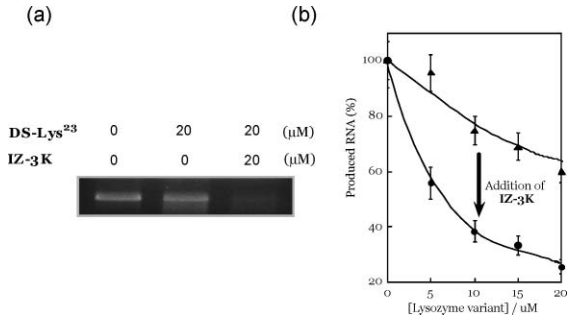

Fig. 9 The inhibition activity of **DS-Lys**[23] in the absence (▲) and presence (●) of **IZ-3K**; [T7 lysozyme variant] = 0–20 μM, [**IZ-3K**] = 0–20 μM, T7 RNAP 5 u, 20 mM rNTP, 10 mM DTT, 2 mM spermidine, 0.01 wt% BSA, 20 mM HEPES (pH 7.9), reaction time 2 hours.

lysozyme variants. However, unfortunately, we could not obtain meaningful heat fluxes for the interaction between **DS-Lys**[23] with T7 RNAP, with or without **IZ-3K**. We could not describe a precise mechanism for regulating T7 RNAP activity using **DS-Lys**[23] and **IZ-3K** from the ITC measurements, but it could be caused by tuning the interaction between T7 RNAP and **DS-Lys**[23], triggered by **IZ-3K** binding.

Conclusion

So far, we have been engaged in the switching-on or -off of natural protein functions by using structural alterations in designed coiled-coil sequences. In the first generation, combination with a circular permutation was required for the target protein, which was demonstrated by the ligand-triggered RNaseT1[11] and metal-ion triggered GFP[12]. But in the second generation, presented here, designing a more specific interaction in the interior of the trimeric coiled-coil sequence, allowed us to construct a ligand-dependent protein by a simple domain insertion. With both methods, to create an "off state", we forced the target protein into a perturbed state by the aid of insertion of a destabilized metamorphosis sequence. With respect to protein folding, the insertion of a destabilized protein domain may retard the folding of the target protein moiety to its original structure possibly causing suppression of its original function. In contrast, enabling the **IZ**-based protein sequences, such as **IZ-DS**, to refold allowed structural alteration in response to an external ligand, **IZ-3K**, even incorporating another protein scaffold. This structural alteration would accelerate and initiate the refolding of the target protein moiety. But the feasibility of our concept, allowing a large fluctuation in target protein activity by ligand addition, would depend on the facility of refolding of the target protein, and restoration of activity to a degree comparable with that of the original protein was hardly reached. In the case of **DS-Lys**[23], the fluctuation of protein function by ligand binding was more than about 7-fold, but the recovered inhibition activity was about 1.4% compared with that of wild-type T7 lysozyme. To overcome this dilemma, we are now examining other methods.

In summary, by designing the metamorphosis peptide **IZ-DS** sequence and the counterpart peptide **IZ-3K** based on the **IZ** sequence, and optimizing the introduction site for the **IZ-DS** sequence to the T7 lysozyme, we succeeded in tuning the interaction between T7 RNAP and T7 lysozyme, resulting in regulation of the RNA synthesis of T7 RNAP. Manipulation of protein–protein interactions by external specific ligands remains one of the important targets in protein engineering. Our method illustrates the possibility of a rational approach to the tuning of protein–protein interactions.

Experimental

Taq DNA polymerase, restriction enzymes, T4 DNA ligase and alkaline phosphatase were purchased from Takara Shuzo, Japan. General chemicals, isopropyl-β-*D*-thiogalacto-pyranoside (IPTG), bacto tryptone, agar, and yeast extract (Wako Chemicals, Japan), ampicillin (Meiji Seika, Japan), Agarose ME (Iwai Chemicals, Japan), glycogen (Roche Diagnostics, Japan) and reagents were used without further purification.

Expression and purification of the wild-type T7 lysozyme and its variants containing the α-helical coiled-coil

The DNA fragments, with NcoI and HindIII restriction enzyme sites at each end, encoding the T7 lysozyme or its mutants fused with coiled-coils, **IZ-DS**, **IZ-DC**, and **IZ-A4** were inserted into the pET-21d(+) vector (Novagen). *E. coli* BL21(DE3) cells were transformed with each plasmid, and were cultured at 37 °C for 3 h in 250 ml of LB medium, and then at 25 °C for 12 h in the presence of 1 mM IPTG. The cells were harvested, resuspended in 7 ml of 20 mM Tris·HCl (pH 7.5) buffer, containing 2 M urea, and sonicated. The suspension was centrifuged, and the supernatant fraction was separated. The supernatant was applied to a His-Bind Resin column (Novagen) (3 ml). The resin was washed with 20 mM Tris·HCl (pH 7.9) buffer (30 ml) containing 500 mM NaCl and 5 mM imidazole, and then with the same buffer containing 500 mM NaCl and 60 mM imidazole (50 ml). The target protein was eluted with the same buffer containing 1 M imidazole (20 ml), and each fraction was analyzed by 15% SDS-PAGE. The fractions containing the target protein were collected, and this solution was dialyzed five times against 1 L of 20 mM Tris·HCl (pH 7.5) containing 50 mM NaCl at 4 °C. Refolding was carried out by slow dilution of the denaturing agent, urea, in the 8 M urea solution, containing 0.1 mM dithiothreitol (DTT) of each protein. The concentration of each protein solution was determined by the A_{280} values in a 6 M guanidine hydrochloride solution, using the ε_{280} values, 26700 M^{-1} cm^{-1} for **WT-Lys**, 26700 M^{-1} cm^{-1} for **DS-Lys**[23] and **A4-Lys**[23], and 29300 M^{-1} cm^{-1} for **DC-Lys**[23], respectively[24].

Circular dichroism (CD) measurement

All CD measurements were carried out on a JASCO J-820 spectrometer, with a 2 mm path length cuvette. The CD spectra of prepared proteins (2.5 or 10 μM) were measured in 20 mM Tris·HCl buffer (pH 7.5) containing 50 mM NaCl. The mean residue ellipticity, $[\theta]$, is given in units of deg cm^2 $dmol^{-1}$. Thermal transition curves were obtained by monitoring $[\theta]_{222}$ as a function of temperature with a 2 mm path length cuvette. The protein concentration was 20 μM, and the temperature was increased at a rate of 1 °C/min. To determine each T_m value from the respective thermal denaturation data of $[\theta]_{222}$, we applied the method described by J. W. Bryson *et al.*[25]

In vitro RNA synthesis of T7 RNA polymerase in the presence of T7 lysozyme variants

Evaluation of the inhibition activities of T7 lysozyme variants was performed using the standard *in vitro* RNA translation kit, supplied by PROMEGA Co. Ltd. An 80 mM HEPES (pH 7.5) solution (20 μL) containing 50 ng of linearized DNA, encoding luciferase (1800 bp), and 5 u of T7 RNA polymerase (invitrogen), T7 Lysozyme variants (0–20 μM), rNTP (5 mM each), 1 u of RNase inhibitor (invitrogen), 24 mM $MgCl_2$, 2 mM spermidine, 40 mM dithiothreitol and 0.01 wt% BSA was incubated for 2 h at 37 °C. To digest template DNA, 10 u of DNaseI was added and the solution was incubated for 15 min at 37 °C. Then, it was mixed with phenol/chloroform (1/1) solution. After centrifugation, the upper fraction was separated and treated by ethanol precipitation. The precipitate was dissolved in 10 μL of DEPC water, containing 3.8 μL of RNA loading buffer and 18 μL of RNA sample buffer and incubated for 10 min at 70 °C. This was subjected to 1% agarose gel electrophoresis and the fluorescence intensity of the produced RNA band was analyzed using Shion-Image software.

Surface plasmon resonance (SPR) measurements

A Biacore biosensor system, Biacore 2000 (GE Healthcare Bioscience, Uppsala, Sweden), was used to measure real-time interactions of **IZ-3K** with **DS-Lys**[23] or **IZ-DS**. Biotinylated **IZ-3K** was immobilized to the sensor chip, SA. **DS-Lys**[23] or **IZ-DS** of various concentrations in PBS containing 0.005% Tween20 were applied over the sensor chip at a rate of 20 μl/min over 3 min. The surface was regenerated with one 15 ml injection of a solution of 3 M guanidine hydrochloride containing 1 M acetic acid. All experiments were performed at 25 °C. The obtained sensorgrams were examined by first adjusting for background changes reflected by the bulk refractive index, and next analyzed kinetically using the BIAevaluation 3.2 software, kinetically. In this program, a global fitting method was used to determine the association and dissociation rate constants, k_{on} and k_{off}, using a model of 1:1 Langmüir binding. The equilibrium association constant, K_a, was calculated from the two rate constants using the equation, $K_a = k_{on} / k_{off}$.

Isothermal titration calorimetry (ITC) measurement

ITC experiments were carried out using a VP-ITC (MicroCal) calorimeter interfaced with a microcomputer. All T7 lysozyme variants were in 100 mM Tris·HCl (pH 8.0) containing 400 mM NaCl, and all solutions were thoroughly degassed using the degassing equipment provided with the instrument. The T7 RNAP solution was titrated into the T7 lysozyme variant solutions (20 μM). Each titration of T7 RNAP solution consisted of a preliminary 2 μL injection followed by 23 subsequent 5 μL additions, which were performed over 10 s periods at 240 s intervals. The heat for each injection was subtracted from the dilution heat of the titrant, and each heat correction was divided by the number of moles of ligand injected. Data were analyzed using the Origin software supplied by MicroCal.

ATR-FTIR measurement

The sample solution was placed on the surface of a diamond ATR crystal (DurasamplIR II, Smiths Detection, 9 effective internal reflections). To regulate the sample temperature, we supplied a glass jacket with circulating water from a low-temperature thermostat (ECOLINE Staredition RE104, LAUDA) on the ATR accessory. The temperature was kept at 23 °C during the measurements. ATR-FTIR spectra of the sample solutions were recorded with 2 cm^{-1} resolution by a Bio-Rad FTS-6000 spectrometer, equipped with a liquid-nitrogen-cooled MCT-detector.[26] The spectra were constructed from 256 interferograms, and six spectra were averaged to improve the signal to noise ratio. The spectra of the buffer solutions were used as background spectra to remove the infrared absorption from water, buffer, *etc.*

Acknowledgements

We gratefully acknowledge the support of a grant-in-aid for Young Scientists (B) from the Japan Society for the Promotion of Science (JSPS), a grant-in-aid for Science Research on Priority Areas "Lifesurveyor" from the Ministry of Education, Culture, Sports Science and Technology of Japan (MEXT), and the INAMORI foundation. We thank Mr. B. Andrew for helpful discussions.

Notes and references

1 (*a*) I. Hamachi, R. Eboshi, J. Watanabe and S. Shinkai, *J. Am. Chem. Soc.*, 2000, **122**, 4530–4531; (*b*) T. Kiwada, K. Sonomura, Y. Sugiura, K. Asami and S. Futaki, *J. Am. Chem. Soc.*, 2006, **128**, 6010–6011; (*c*) J. Liang, J. R. Kim, J. T. Boock, T. J. Mansell and M. Ostermeier, *Protein Sci.*, 2007, **16**, 929–937.
2 M. Dalmau, S. Lim and S. Wang, *Nano Lett.*, 2009, ASAP.
3 (*a*) K. Curley and D. S. Lawrence, *Curr. Opin. Chem. Biol.*, 1999, **3**, 84–88; (*b*) D. S. Lawrence, *Curr. Opin. Chem. Biol.*, 2005, **9**, 570–575; (*c*) Y. Shigeri, Y. Tatsu and N. Yumoto, *Pharmacol. Ther.*, 2001, **91**, 85–92; (*d*) D. M. Rothman, E. J. Petersson, M. E. Vzquez, G. S. Brandt, D. A. Dougherty and B. Imperiali, *J. Am. Chem. Soc.*, 2005, **127**, 846–847; (*e*) M. E. Vzquez, M. Nitz, J. Stehn, M. B. Yaffe and B. Imperiali, *J. Am. Chem. Soc.*, 2003, **125**, 10150–10151; (*f*) G. A. Woolley, *Acc. Chem. Res.*, 2005, **38**, 486–493; (*g*) G. A. Woolley, A. S. I. Jaikaran, M. Berezovski, J. P. Calarco, S. N. Krylov, O. S. Smart and J. R. Kumita, *Biochemistry*, 2006, **45**, 6075–6084; (*h*) N. Wu, A. Deiters, T. A. Cropp, D. King and P. G. Schultz, *J. Am. Chem. Soc.*, 2004, **126**, 14306–14307; (*i*) K. Zou, S. Cheley, R. S. Givens and H. Bayley, *J. Am. Chem. Soc.*, 2002, **124**, 8220–8229.
4 (*a*) H. E. Hoffman, E. R. Blair, J. E. Johndrow and A. C. Bishop, *J. Am. Chem. Soc.*, 2005, **127**, 2824–2825; (*b*) X. Zhang and A. C. Bishop, *J. Am. Chem. Soc.*, 2007, **129**, 3812–3813.
5 (*a*) G. Guntas and M. Ostermeier, *J. Mol. Biol.*, 2004, **336**, 263–273; (*b*) M. Ostermeier, *Protein Eng. Des. Sel.*, 2005, **18**, 359–364.
6 H. D. Mootz and T. W. Muir, *J. Am. Chem. Soc.*, 2002, **124**, 9044–9045.
7 (*a*) A. N. Lupas and M. Gruber, *Adv. Protein. Chem.*, 2005, **70**, 37–78; (*b*) D. N. Woolfson, *Adv. Protein Chem.*, 2005, **70**, 79–112; (*c*) P. Burkhard, J. Stetefeld and S. V. Strelkov, *Trends Cell Biol.*, 2001, **11**, 82–88; (*d*) A. Lupas, *Trends Biochem. Sci.*, 1996, **21**, 375–382.
8 K. Suzuki, H. Hiroaki, D. Kohda and T. Tanaka, *Protein Eng.*, 1998, **11**, 1051–1055.
9 B. Tripet, K. Wagschal, P. Lavigne, C. T. Mant and R. S. Hodges, *J. Mol. Biol.*, 2000, **300**, 377–402.
10 A. Kashiwada, H. Hiroaki, D. Kohda, M. Nango and T. Tanaka, *J. Am. Chem. Soc.*, 2000, **122**, 212–215.
11 T. Kiyokawa, K. Kanaori, K. Tajima, M. Kawaguchi, T. Mizuno, J. Oku and T. Tanaka, *Chem. Eur.*, 2004, **10**, 3548–3554.
12 S. Yuzawa, T. Mizuno and T. Tanaka, *Chem.–Eur. J.*, 2006, **12**, 7345–7352.
13 T. Mizuno, K. Murao, Y. Tanabe, M. Oda and T. Tanaka, *J. Am. Chem. Soc.*, 2007, **129**, 11378–11383.
14 K. Lugar, U. Hommel, M. Herold, J. Hofsteenge and K. Kirschner, *Science*, 1989, **243**, 206–219.
15 M. M. G. Krishna and W. Englander, *Proc. Natl. Acad. Sci. U. S. A.*, 2005, **102**, 1053–1058.

16 (*a*) X. Cheng, X. Zhang, J. W. Pflugrath and F. W. Studier, *Proc. Natl. Acad. Sci. U. S. A.*, 1994, **91**, 4034–4038; (*b*) D. Jeruzalmi and T. A. Steitz, *EMBO J.*, 1998, **17**, 4101–4113; (*c*) A. Kumar and S. S. Patel, *Biochemistry*, 1997, **36**, 13954–13962.
17 (*a*) K. Suzuki, T. Yamada and T. Tanaka, *Biochemistry*, 1999, **38**, 1751–1756; (*b*) K. Wada, T. Mizuno, J. Oku and T. Tanaka, *Protein Peptide Lett*, 2003, **10**, 27–33.
18 (*a*) X. Li, K. Suzuki, K. Tajima, A. Kashiwada, H. Hiroaki, D. Kohda and T. Tanaka, *Protein Sci.*, 2000, **9**, 1327–1333; (*b*) M. Koike, K. Wada, T. Kiyokawa, K. Kanaori, K. Tajima, T. Mizuno, J. Oku and T. Tanaka, *Peptide Science*, 2003, **2002**, 355–356; (*c*) T. Kiyokawa, K. Kanaori, K. Tajima, M. Koike, T. Mizuno, J. Oku and T. Tanaka, *J. Pept. Res.*, 2004, **63/4**, 347–354; (*d*) T. Tanaka, T. Mizuno, S. Fukui, H. Hiroaki, J. Oku, K. Kanaori, K. Tajima and M. Shirakawa, *J. Am. Chem. Soc.*, 2004, **126**, 12043–12048.
19 (*a*) B. Ciani, E. G. Hutchinson, R. B. Sessions and D. N. Woolfson, *J. Biol. Chem.*, 2002, **277**, 10150–10155; (*b*) M. J. Pandya, E. Cerasoli, A. Joseph, R. G. Stoneman, E. Waite and D. N. Woolfson, *J. Am. Chem. Soc.*, 2004, **126**, 17016–17024; (*c*) E. Cerasoli, B. K. Sharpe and D. N. Woolfson, *J. Am. Chem. Soc.*, 2005, **127**, 15008–15009; (*d*) X. I. Ambroggio and B. Kuhlman, *J. Am. Chem. Soc.*, 2006, **128**, 1154–1161.
20 N. Doi and H. Yanagawa, *FEBS Lett.*, 1999, **457**, 1–4.
21 (*a*) S. Nautiyal, D. N. Woolfson, D. S. King and T. Alber, *Biochemistry*, 1995, **34**, 11645–11651; (*b*) D. M. Eckert, V. N. Malashkevich and P. S. Kim, *J. Mol. Biol.*, 1998, **284**, 859–865.
22 D. L. Vien, N. B. Colthup, W. G. Fateley and J. G. Grasselli, *The Handbook of Infrared and Raman Characteristic Frequencies of Organic Molecules*, Academic Press, 1991.
23 P. B. Harbury, T. Zhang, P. S. Kim and T. Alber, *Science*, 1993, **262**, 1401–1407.
24 J. E. Coligan, B. M. Dunn, D. W. Speicher and P. T. Wingfield, *Short Protocol in Protein Science*, Wiley, 2003.
25 J. W. Bryson, J. R. Desjarlais, T. M. Handel and W. F. DeGrado, *Protein Sci.*, 1998, **7**, 1401–1414.
26 Y. Kitade, Y. Furutani, N. Kamo and H. Kandori, *Biochemistry*, 2009, **48**, 1596–1603.